AIP | The Journal of Chemical Physics

Glass transition dynamics and conductivity scaling in ionic deep eutectic solvents: The case of (acetamide + lithium nitrate/sodium thiocyanate) melts

Satya N. Tripathy, Zaneta Wojnarowska, Justyna Knapik, Hideaki Shirota, Ranjit Biswas, and Marian Paluch

Citation: The Journal of Chemical Physics **142**, 184504 (2015); doi: 10.1063/1.4919946
View online: http://dx.doi.org/10.1063/1.4919946
View Table of Contents: http://scitation.aip.org/content/aip/journal/jcp/142/18?ver=pdfcov
Published by the AIP Publishing

Glass transition dynamics and conductivity scaling in ionic deep eutectic solvents: The case of (acetamide + lithium nitrate/sodium thiocyanate) melts

Satya N. Tripathy,[1,2,a)] Zaneta Wojnarowska,[1,2] Justyna Knapik,[1,2] Hideaki Shirota,[3] Ranjit Biswas,[4] and Marian Paluch[1,2]

[1]*Institute of Physics, University of Silesia, Uniwersytecka 4, 40-007 Katowice, Poland*
[2]*Silesian Center for Education and Interdisciplinary Research, 75 Pulku Piechoty 1A, 41-500 Chorzow, Poland*
[3]*Department of Nanomaterial Science and Department of Chemistry, Chiba University, 1-33 Yayoi, Inage-ku, Chiba 263-8522, Japan*
[4]*Department of Chemical, Biological and Macromolecular Sciences, S. N. Bose National Centre for Basic Sciences, JD Block, Sector III, Salt Lake, Kolkata 700098, India*

(Received 24 December 2014; accepted 28 April 2015; published online 13 May 2015)

A detailed investigation on the molecular dynamics of ionic deep eutectic solvents (acetamide +lithium nitrate/sodium thiocyanate) is reported. The study was carried out employing dielectric relaxation spectroscopy covering seven decades in frequency (10^{-1}-10^{6} Hz) and in a wide temperature range from 373 K down to 173 K, accessing the dynamic observables both in liquid and glassy state. The dielectric response of the ionic system has been presented in the dynamic window of modulus formalism to understand the conductivity relaxation and its possible connection to the origin of localized motion. Two secondary relaxation processes appear below glass transition temperature. Our findings provide suitable interpretation on the nature of secondary Johari-Goldstein process describing the ion translation and orientation of dipoles in a combined approach using Ngai's coupling model. A nearly constant loss feature is witnessed at shorter times/lower temperatures. We also discuss the ac conductivity scaling behavior using Summerfield approach and random free energy barrier model which establish the time-temperature superposition principle. These experimental observations have fundamental importance on theoretical elucidation of the conductivity relaxation and glass transition phenomena in molten ionic conductors. [http://dx.doi.org/10.1063/1.4919946]

I. INTRODUCTION

The time evolution of cooperatively relaxing systems is a robust area of research for decades.[1–10] These systems include all kinds of glass forming supercooled liquids and molten ionic conductors which offer potential applications in the field of material chemistry.[1–10] The phenomenon of glass transition involves slowing down of cooperative relaxing units from the order of picoseconds ($\approx 10^{-12}$ s) in the supercooled liquid state to the macroscopic times ($\approx$100 s) in the glassy state.[6] The measurement of different dynamic observables such as viscosity, dielectric relaxation time, and conductivity as a function of thermodynamic intensive parameters provides the quantitative description of cooperative relaxation.[1–11] In this context, the dielectric relaxation spectroscopy is the appropriate experimental tool to probe and understand the molecular dynamics of the glass forming systems in a large time window. Among the ionic conductors, deep eutectic solvents (DESs) exhibit similar physico-chemical properties to the conventionally used room temperature ionic liquids (RTILs).[12–20] These are mixture of ionic and non-ionic solid compounds which form a eutectic with a melting point much lower than either of the individual components. Therefore, in recent years many new DESs have been rapidly designed as green solvents that have several desired properties, such as poor conductivity, high viscosity, low vapor pressure, and high thermal stability.[15–17,21,22]

Aside from the importance of DESs in novel applications, a lesser attention has been devoted to the experimental investigations on the fundamental aspects of glass transition and ionic conductivity relaxation. In particular, when acetamide (CH_3CONH_2) mixed with inorganic salts yield liquids near room temperature with outstanding affinity to supercool and has unique solvating feature.[23–26] Moreover, the supercooling phenomenon also depends on the nature of the ion content in the mixture. Acetamide is dielectrically rigid and exhibits non-centrosysmmetric molecular ordering that permits high dipole moment of magnitude 3.7 D in the molecule.[27] Ultimately, the studies of dielectric relaxations concerning rigid character of the molecules hold the fundamental interest in glass transition which falls into the special class of Johari-Goldstein (JG) secondary relaxations.[28–34] Apart from dielectric studies, NMR spectroscopy and mechanical relaxations also support the evidence of secondary relaxations.[10] Rossler and coworkers have noted that the glass formers in this class display a common pattern in thermal behavior of secondary relaxation times with activation energy of $E_a \approx 24RT_g$.[11,33] This empirical relation is only approximate and there are still deviations. Later, Ngai and coworkers found more general relation between the activation energy of JG relaxation and T_g of glass formers using coupling model (CM).[33] Nevertheless, the fundamental nature of secondary relaxations in glass forming supercooled liquids

a)Author to whom correspondence should be addressed. Electronic mail: satyanarayantripathy@gmail.com

and ionic conductors is a matter of attention and debate. Again, the secondary JG relaxations in the dielectric spectra of purely ionic systems are also an open question and needs to be addressed.[11,36,37] Recently, Jarosz *et al.* have discussed the possible origin of ionic character of secondary JG relaxation in 1-methyl-3-trimethylsilylmethylimidazolium tetrafluoroborate using Ngai's coupling model and high pressure dielectric studies.[38] Therefore, the examination of these kinds of processes in ionic DESs can lead to a better understanding of their origin. The DESs in the present investigation are binary eutectic mixtures of dipolar acetamide (CH_3CONH_2) and lithium nitrate ($LiNO_3$)/sodium thiocyanate (NaSCN). This system exhibits the unique feature of ion conduction in a dipolar solvent that permits ion-ion, dipole-dipole, and ion-dipole interactions which may provide intriguing features in secondary relaxations. In view of the above, it is of a significant interest to study the conductivity and secondary relaxation processes in these ionic DESs. Until now, a systematic investigation on the molecular dynamics of these ionic DESs has not been carried out using dielectric spectroscopy, although a few studies involving fast spectroscopic measurements and computer simulations have been initiated in recent years to explore the interaction and dynamics of the multi-component ionic systems by Biswas and co-workers.[39–42] In addition, the dielectric relaxation, density, and viscosity of CH_3CONH_2–NaSCN eutectic mixtures have also been reported.[26,43,44]

In this communication, we present a systematic analysis of the dielectric relaxation behavior of DESs: $0.78CH_3CONH_2 + 0.22LiNO_3$ and $0.75CH_3CONH_2 + 0.25NaSCN$, over a wide temperature and frequency range with the aim to understand the conductivity relaxation and secondary processes. To describe the ion dynamics of the DESs, we have adopted the complex electrical modulus $M^*(\upsilon)$ and complex conductivity $\sigma^*(\upsilon)$ functions. Emphasis has been put to recognize and resolve the ionic nature of JG secondary relaxation process which is still under debate. We also provide scaling analysis for the ac conductivity spectra using Summerfield approach and free energy random barrier model developed by Dyre.[6]

II. EXPERIMENTAL

The crystalline form of acetamide (CH_3CONH_2) (purity ≥ 99%), lithium nitrate ($LiNO_3$) (purity ≥ 99.5%), and sodium thiocyanate (NaSCN) (purity > 99%) was purchased from Sigma Aldrich and used as received. To prepare the deep eutectic solvents with the composition $0.75CH_3CONH_2 + 0.25NaSCN$ (abbreviated as DES-Na) and $0.78CH_3CONH_2 + 0.22LiNO_3$ (abbreviated as DES-Li), the quench cooling technique was applied. To obtain the homogeneous mixtures, first we thoroughly mixed crystalline powders of both compounds in appropriate proportions in a heat-resistant glass vial (weight of acetamide + NaSCN was 6.645 g + 3.040 g, while acetamide + $LiNO_3$ was 6.911 g + 2.275 g). After that, we put the magnetic stir bar into a vial with each mixture. Next, the crystalline mixture samples were melted in the vial on the hot plate magnetic stirrer (CAT M 17.5) at around 353 K. The temperature inside the vials was controlled by using a Pt-100 sensor. Only when the mixtures were fully melted the magnetic mixing (about 500 rpm) was switched on. After about 5 min of magnetic stirring of the liquids we obtained homogeneous mixtures. The whole sample preparation procedure was carried out in a humidity controlled glove box (PLAS LABORATORIES, Inc. 890-THC-DT/EXP/SP) at the assured relative humidity RH < 5%. The samples obtained in this way were measured immediately after the preparation to protect them from atmospheric moisture.

For the dielectric measurements DES-Li and DES-Na, samples were placed between two stainless steel electrodes of the capacitor. The dielectric spectra were collected over a wide frequency (10^{-1}–10^6 Hz) and temperature range (from 173 to 373 K) using a Novo-Control GMBH Alpha dielectric spectrometer. The temperature was controlled by the Novo-Control Quattro system, with the use of a nitrogen gas cryostat. Temperature stability was better than 0.1 K. Differential Scanning Calorimetry (DSC): Calorimetric measurements of examined DES were performed with a Mettler-Toledo DSC apparatus equipped with a liquid nitrogen cooling accessory and an HSS8 ceramic sensor (heat flux sensor with 120 thermocouples). Temperature and enthalpy calibrations were carried out by using indium and zinc standards. The DES-Li sample was placed in aluminum crucible (40 μl) and scanned at a rate of 10 K/min over a temperature range from 173 K to 373 K.

III. RESULTS AND DISCUSSION

A. Molecular dynamics above glass transition

In case of ionic conductors at sufficiently low frequencies, cooperative ion hopping dominantly influences the dielectric measurements in complex permittivity; $\varepsilon^*(\upsilon) = \varepsilon'(\upsilon) - i\varepsilon''(\upsilon)$ or equivalently in the complex conductivity; $\sigma^*(\upsilon) = \sigma'(\upsilon) + i\sigma''(\upsilon)$ formalism.[9,45,46] This feature is reflected by a sharp increase in the dielectric loss function, $\varepsilon''(\upsilon)$ at low frequency that entirely masks the structural relaxation process. Therefore, in order to present the dielectric data more conveniently for molten ionic conductors, we have adopted electric modulus, $M^*(\upsilon)$ formalism which connects the above mentioned two representations by the following relation:[45,46]

$$M^*(\upsilon) = \frac{1}{\varepsilon^*(\upsilon)} = \frac{i2\pi\upsilon\epsilon_0}{\sigma^*(\upsilon)}, \tag{1}$$

where ϵ_0 is the permittivity of vacuum and υ corresponds to frequency. Ultimately for ionic conductors, the most appropriate data presentation is not dielectric loss function $\varepsilon^*(\upsilon)$ but the complex electric modulus $M^*(\upsilon)$ approach. $M^*(\upsilon)$ formalism signifies ion conductivity relaxation which differs from dipole relaxation in supercooled liquids. Physically, the electric modulus relates to the relaxation of the electric field **E** in the material when the electric displacement vector **D** remains constant, i.e., $\mathbf{E}(t) = \mathbf{E}(0)\Phi(t)$.[3] Consequently, $M^*(\upsilon)$ formalism implies the real dielectric relaxation process. On the contrary, the dielectric permittivity $\varepsilon^*(\upsilon)$ mirrors the relaxation of the electric displacement vector when the electric field remains constant. So, the susceptibility representation

describes the dielectric retardation process. The frequency dependence of the complex electric modulus $M^*(\upsilon)$ comes from the time dependence of the correlation function φ(t) of ion motion via the Fourier transform[3]

$$M^* = M'(\upsilon) + iM''(\upsilon) = M_\infty \left[1 - \int_0^\infty dt \exp(-i\upsilon t)\left(-\frac{d\phi}{dt}\right)\right]. \quad (2)$$

Here, M_∞ is the reciprocal of the high frequency dielectric constant ε_∞ and Φ(t) is the relaxation function, represented by the Kohlrausch-Williams-Watts (KWW) function[47–49]

$$\phi_{KWW} = \exp\left[-\left(\frac{t}{\tau_\alpha}\right)^{1-n}\right]. \quad (3)$$

In the absence of interaction between the ions, Φ(t) is a simple exponential decay function, resulting $M''(\upsilon)$ a symmetric Debye peak with full width half maxima equal to 1.14 decade in frequency. Here, τ_α is the α-conductivity relaxation time and the fractional quantity, $0 < n < 1$, in the exponent is the measure of interaction and correlation.

Fig. 1 illustrates the dielectric response of DES-Li and DES-Na melts measured over seven decades of frequency (10^{-1}-10^6 Hz) in a wide temperature range (173 K-373 K) in both modulus, M″(υ) and conductivity, σ′(υ) representation at ambient pressure. It is observed that the imaginary part of complex modulus appears as a well-pronounced peak, so-called a conductivity relaxation peak. On the other hand, the real part of the complex conductivity, σ′(υ) is characterized on the low frequency side by a plateau (i.e., dc conductivity, σ_{dc}) and the power law behavior proposed by Jonscher at higher frequencies.[50] In this context, it is important to note that the dc-conductivity provides the direct information of ion hopping which is equal to the product of the number of ions and their mobility. The dc conductivity is inversely related to the relaxation times (τ_M) estimated from the frequency of M″ peak maximum. In Figs. 1(a) and 1(b), the experimental window of M″(υ) clearly shows the existence of three relaxation processes: (i) the spectra recorded from 173 K to 215 K display two well defined secondary relaxations, corresponding to some localized motions that move toward high frequencies with increasing temperature for both the glass formers, (ii) then, asymmetric conductivity relaxation peak appearing from

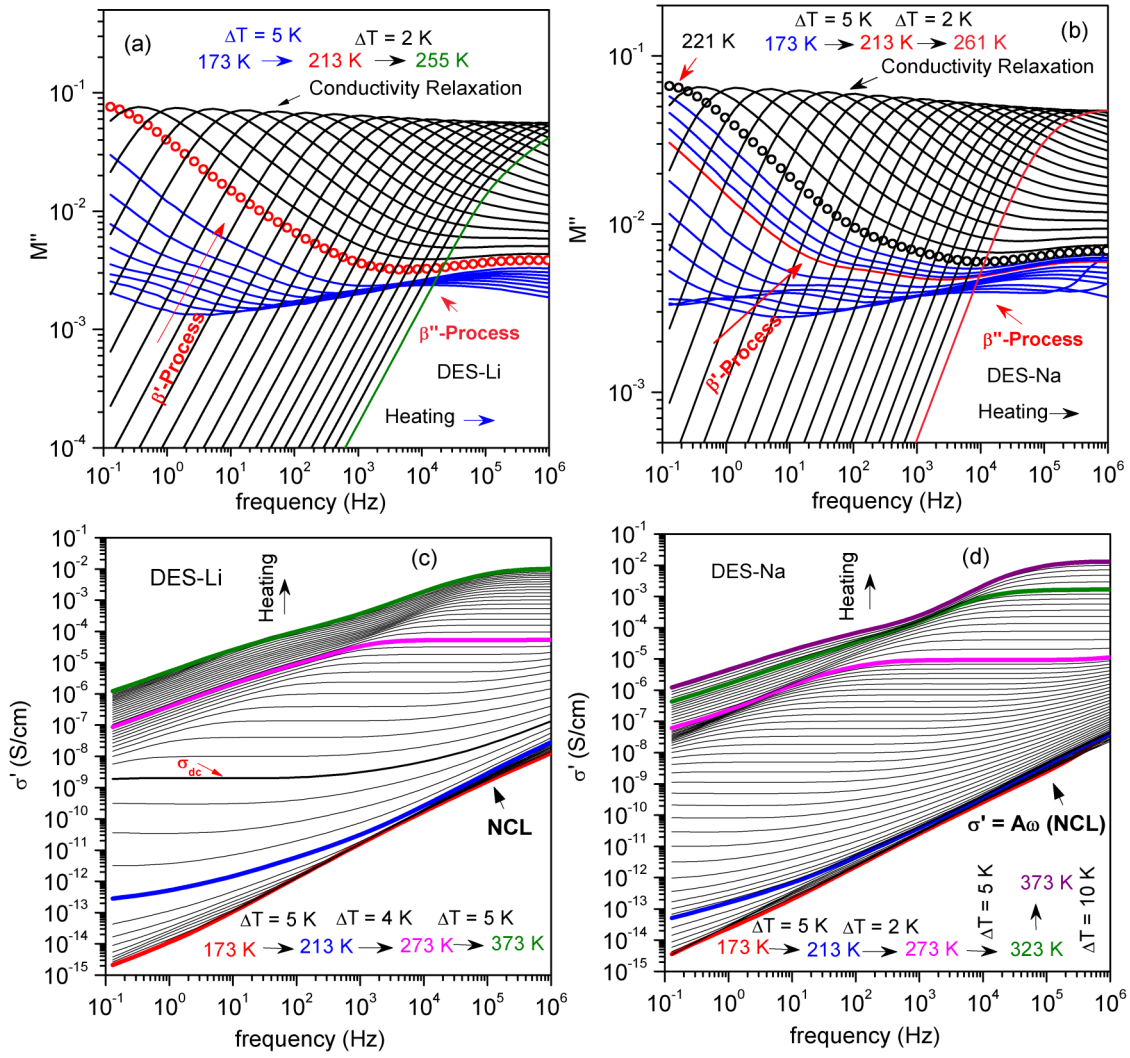

FIG. 1. (a) and (b) Imaginary part of the complex electric modulus, M″(υ) and (c) and (d) real part of complex conductivity σ′(υ) as a function of frequency and temperature, spanning across glass transition temperature, T_g of DES-Li and DES-Na.

the ion migration becomes the central feature in the modulus spectra which moves towards high frequency side with increasing temperature. The M″(υ) peak maximum is observed in the experimental window up to 273 K and after that data have been presented in conductivity formalism. The analysis of dielectric data in conductivity representation will be discussed in later sections. The conductivity relaxation peak appears as an asymmetric profile that exhibits width broader than the Debye peak.[6] The asymmetric power-law behavior of the modulus data at low and high frequencies, shown in Figs. 1(a) and 1(b) suggests that conductivity relaxation can be appropriately modeled by the *Havriliak-Negami* (HN)[51] relaxation function, $F^*_{HN}(\omega)$ which takes the mathematical form

$$F^*_{HN}(\omega) = \frac{1}{[1 + (i\omega\tau_{HN})^{\alpha}]^{\beta}}, \tag{4}$$

where τ_{HN} defines a characteristic relaxation time and the shape parameters, α and β are related to $(1 - n) = \beta_{KWW}$ by the equation[6,13]

$$\alpha\beta = [\beta_{KWW}]^{1.23}. \tag{5}$$

Using HN fittings, we have calculated the following dynamic parameters from the M″(υ) spectra: (a) the dc conductivity from the low-frequency region of $\sigma' \approx \frac{2\pi\upsilon\epsilon_0}{M''}$; (b) the σ-conductivity relaxation time, and (c) two secondary β-relaxation times from the frequency corresponding to the M″ maximum $\tau = \frac{1}{2\pi\upsilon_{max}}$. To further advance our understanding of the charge transport and using the information from the HN fits, we have constructed the relaxation map of both the glass formers by plotting $\log\tau$ and $\log\sigma_{dc}$ as function of 10^3/T for primary conductivity and secondary relaxation process as shown in Fig. 2. This relaxation map mirrors the dynamic properties of the glass formers and is the central feature of our investigation. In this section, we discuss only the conductivity relaxation above glass transition. The glass transition temperature has been determined from calorimetric studies (standard heating rate: 10 K/min) which corroborates with dielectric relaxation time at $\tau = 1$ s (cf. Fig. 2-inset). From the dielectric data, the glass transition temperatures, T_g of the DES-Li and DES-Na are estimated to be around 213 K and 221 K, respectively. The temperature dependence of conductivity relaxation times, τ_σ and σ_{dc} are found to obey single Vogel-Fulcher-Tamann (VFT) feature and its mathematical relation is given by[52–54]

$$\log\tau_\sigma = \log\tau_\infty + \frac{DT_0}{T - T_0}\log\tau_e, \tag{6}$$

where D is the fragility parameter which quantifies the divergence from Arrhenius behavior, T_0 is the Vogel temperature, and τ_∞ is the limiting relaxation time at high temperature. The temperature dependences of σ_{dc} and τ_σ are found to be almost the same. The estimated VFT parameters have been listed in Table I. Here, it is worth noting that the D-value of DES-Li is more than DES-Na suggesting opposite behavior in fragility parameter. This increase in fragility due to the change of ion-type can be explained by the increase in degree of cooperative motion in the system.[55] We also found an existence of crossover from VFT to Arrhenius behavior which suggests that macroscopic ion transport does not completely mimic the structural relaxation. Rather, there exists a decoupling between

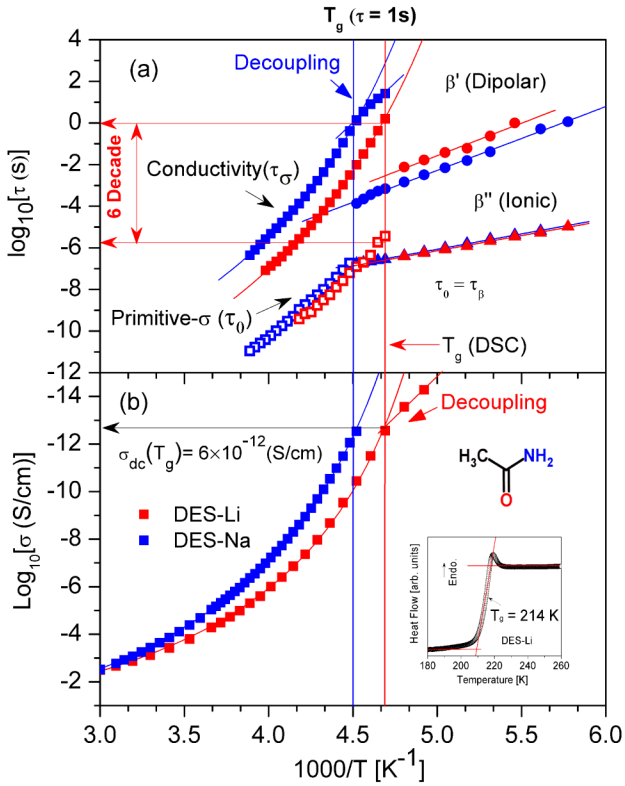

FIG. 2. Relaxation map: Temperature dependence of (a) relaxation times ($\log\tau$) and (b) dc-conductivity ($\log\sigma_{dc}$) as a function of $\frac{1000}{T}$ of DES-Li and DES-Na. The solid lines correspond to fits to the experimental data.

them at conductivity relaxation time equal to $\tau = 1$ s which is the manifestation of liquid-glass transition. According to the convention, the ionic conductivity in a system where the conductivity relaxation is strongly coupled to the structural relaxation is in the order of $\sim 10^{-15}$ S/cm at T_g.[56] However, the $\sigma_{dc}(T_g)$ estimated for the examined herein ionic melts is several orders of magnitude higher than this value (6×10^{-12} S/cm).

In order to monitor the shape of the conductivity relaxation profile as a function of temperature, we have constructed the master curve by superimposing a number of dielectric modulus profiles recorded at different temperatures (i.e., above and below T_g), to the spectrum obtained at T = 217.15 K; for DES-Li and T = 225.15 K; for DES-Na as the reference (see Fig. 3). The obtained master plot clearly shows that the shape of the conductivity-profile is practically invariant upon heating. This observation provides the evidence to support the time-temperature superposition in the present examined materials. In Sec. III C, we provide a compressive discussion on conductivity scaling using Summerfield and Dyre models.[6]

B. Molecular dynamics below glass transition

When the intensive parameter drives the ionic melt from liquid to glassy state, all the global cooperative motions are arrested and amplification of localized process takes place in the experimental window within the temperature range 173-215 K as shown in Figs. 1(a) and 1(b). These local motions are known as secondary relaxation processes. In the present glass former, we notice two secondary processes, one at low frequency (denoted as β′-process) and another at high frequency

TABLE I. VFT fit parameters of conductivity relaxation-σ, dc-conductivity, and Arrhenius parameters of secondary β′, β″ processes.

	σ-process			dc-conductivity			β′-process		β″-process	
	Log τ_0	D	T_0	Log σ_0	D	T_0	Log τ_0	E_a (kJ/mol)	Log τ_0	E_a (kJ/mol)
DES Li	−18.90 ± 0.59	18.08 ± 1.73	151.14 ± 2.88	−1.47 ± 0.05	8.20 ± 0.14	176.62 ± 0.51	−16.18 ± 1.19	59.77 ± 4.47	−13.42 ± 0.14	27.90 ± 0.54
DES Na	−16.43 ± 0.22	13.09 ± 0.54	164.69 ± 1.18	−0.57 ± 0.09	6.04 ± 0.2	178.16 ± 0.8	−17.61 ± 0.26	58.69 ± 1.00	−13.45 ± 0.06	28.28 ±0.26

(denoted as β″) below T_g. Both the secondary relaxations move towards higher frequency side on increasing temperature. With the purpose of understanding the origin of these processes, we have characterized the local processes by their dynamic properties. In order to analyze and interpret the thermal behavior of secondary relaxation, we have plotted the characteristic times, $\tau = \frac{1}{2\pi\upsilon_{max}}$ as function of 10^3/T (see Fig. 2). Both the secondary processes obey the Arrhenius law and the mathematical relation is given by

$$\log \tau = \log \tau_\infty + \frac{E_a}{RT} \log \tau_e, \tag{7}$$

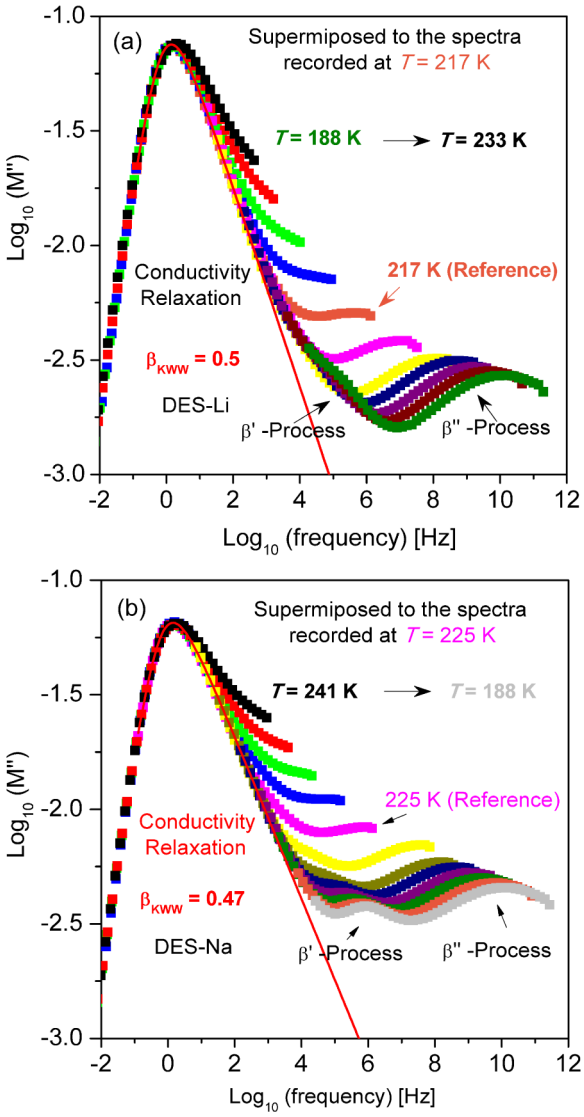

FIG. 3. Master curve: Superimposed dielectric modulus spectra of (a) DES-Li and (b) DES-Na, at seven different temperatures above and below T_g. The solid red line represents the HN fit.

where τ_∞ is the pre-exponential factor, E_a is the energy barrier/activation energy, and R is the gas constant. The experimental data have been fitted to the above equation and the Arrhenius parameters are listed in Table I. Secondary relaxations abound in glass formers are found using dielectric, mechanical, NMR spectroscopy, and phonon co-related spectroscopy.

The DESs in the present investigation are binary mixtures and comprise of two simple components where matrix is the acetamide (i.e., avg. dimension ≈ 11.5 Å; calculated from the cube root of unit cell volume of rhombohedral crystal structure with *R*3*c* space group)[57] and active ions are (Li^+ ≈ 1.52 Å/Na^+ ≈ 1.98 Å).[58,59] It has been well established that there are two possible molecular origins of secondary relaxation phenomena. The former one is associated with molecular internal degrees of freedom (i.e., intra-molecular). But, the latter one initiates from some local motions of the entire molecule (i.e., inter-molecular; a special case of a rigid unit) which falls into the special class of JG process.[10,33–35] Here, we have adopted the Ngai CM to understand the possible connection of the secondary relaxation processes to the Johari-Goldstein relaxation and the mathematical relation is given by[9]

$$\tau_0 = (t_c)^n (\tau_\sigma)^{1-n}, \tag{8}$$

where τ_0 is the independent/primitive relaxation of the coupling model and the precursor of the cooperative (i.e., intermolecular coupled) global structural relaxation (τ_α). It is a local process and contains motion of all parts of the molecule. Since the dielectric data have been presented in modulus formalism, therefore, the structural relaxation (τ_α) is replaced by conductivity relaxation (τ_σ) in the coupling model. Herein, τ_0 signifies the *primitive conductivity relaxation times* of the CM[38] and t_c is the crossover time from independent relaxation to the cooperative relaxation and ~2 ps for molecular liquids.[9] The CM enables us to estimate the magnitude of τ_0 to be calculated from the KWW function (stretched exponential) that fits the time dependence of the σ-process and interpretation of the evolution of ion dynamics. It is well recognized that the independent relaxation time τ_0 is approximately located near the most probable relaxation time τ_β of the JG relaxation at all values of temperature,[10] i.e,

$$\tau_0(T) \approx \tau_\beta(T). \tag{9}$$

In relaxation map of the DESs, we detect an interesting experimental connection of primitive conductivity relaxation τ_0 to the faster relaxation process $\tau_{\beta''}$ as shown in Fig. 2. Since τ_0 is a precursor of primary conductivity relaxation, involves macroscopic ion transport and intermolecular in nature, we expect that β″-process carries similar information, i.e., parallel origin to τ_0. This interesting observation offers the opening mark of ionic nature of fast β″-relaxation which is of JG

kind, i.e., the JG conductivity relaxation due to long range coulomb interaction. Again the CM connects the ratio of the conductivity relaxation and JG relaxation to the breadth of the conductivity relaxation and is mathematically represented as[10]

$$\left(\log \tau_\sigma - \log \tau_{\beta''}\right) \approx n \left(\log \tau_\sigma - \log t_c\right). \quad (10)$$

This relation connects the dynamic properties of σ-process and JG β″-relaxation. This equation also has been verified for large number of glass formers[10] and is consistent with our dielectric data. Performing the simple calculation of σ-process at T_g = 213 K for DES-Li and n = 0.5 (from fitting analysis), we found that $\left(\log \tau_\sigma - \log \tau_{\beta''}\right)$ = 6 decade and $\left(\log \tau_\sigma - \log t_c\right)$ = 11.7 decade in frequency. Similar feature is also noticed in case of DES-Na.

The activation energies of secondary fast processes of DES-Li and DES-Na are found to be 27.9 (±0.54) and 28.28 (±0.26) kJ/mol, respectively.[59] Moreover, the magnitude of activation energies of $\tau_{\beta''}$ process is independent of the ion-type involved. Similar magnitude of activation energy values has also been reported in PEO-Li based systems.[59] It is also interesting to note that both the samples have pre-exponential factor of temperature dependence of characteristic times, i.e., $\log \tau_\infty = 10^{-13}$ s of β″-relaxation which corresponds to the comparable magnitude of primitive conductive relaxation τ_0 at very earlier times.[11] Moreover, this process exhibits a weaker dependence of dielectric strength as can be seen from Figs. 1(a) and 1(b). From conductivity isotherms in the temperature range below 208 K, we also notice nearly constant loss (NCL) behavior at higher frequencies as seen from Figs. 1(c) and 1(d). For ionic conductors where the ions are charged atoms, NCL is a commonly used term to describe loss by $M''(\upsilon) \propto \nu^{-c}$ or $\sigma'(\nu) \propto \nu^{1-c}$, with c being small.[9] The origin of NCL behavior is understood as the motion of ions or molecules in the cage defined by anharmonic intermolecular potential. The NCL has no characteristic time and is not an ordinary relaxation. It transpires at short times and long before the ions or molecules execute local (secondary relaxation) and long range diffusion that give rise to ac and dc conductivities.[9] Plenty of experimental evidence supporting this can be found in the literature.[60–62] To be effective in causing cage decay, this specific secondary relaxation involves short range hop of the ion or locally the rotation and/or translation of the entire molecule, which is distinguished as JG β-relaxation.[10] Evidence of the JG β-relaxation involves local motion of either the ion or the molecule and can be drawn from the magnitude of the activation energy defining the Arrhenius temperature dependence of the JG β-relaxation time in the glassy state. In the present case, the activation energy of the β′-process is about 54 kJ/mol, typical of JG β-relaxation in non-associating molecules, and the activation energy of the β″-process is even smaller because it is for local ionic hop. Naturally, such caged dynamics involve motions with smaller amplitudes and no cooperativity. Apart from that, JG β″-relaxation plays in cage decay resulting in terminating the NCL regime.[9,62]

Now we put our emphasis on the simple calculation of theoretical binding energy (E_b) of contact ion pairs using long range coulomb interaction picture in the acetamide medium and its qualitative interpretations. Here, we have considered a simple model, taking into account Li^+-Acetamide-Li^+ in a one-dimensional construction to calculate E_b. The columbic interaction can be represented mathematically by[6]

$$E_b = \frac{-q^2}{4\pi\varepsilon_0\varepsilon_r d}, \quad (11)$$

where d is the distance between ion pairs and $\varepsilon_r \approx 3.5$ for DES at high frequency in glassy state. Using ionic radius of Li^+/Na^+ (r = 0.76 Å/r = 0.99 Å)[58,59] and avg. diameter of Acetamide, i.e., a = 11.5 Å,[57] the values of E_b surprisingly are found to be ≈30.4 and 29.44 kJ/mol, respectively. The appearance of this magnitude of binding energy is equivalent to the calculated activation energy from temperature dependence of characteristic relaxation time of β″-relaxation process. This simple evidence put strong emphasis on qualitative interpretation about ionic nature of fast relaxation behavior. Therefore, from the above discussion we have tried to provide the resolution on the possible connection of β″-relaxation with long range coulomb interaction of JG kind in the present examined glass formers. Similar types of observation have been reported for high frequency conductive JG relaxation in 1-methyl-3-trimethylsilylmethylimidazolium tetrafluoroborate.[38]

Now, we concentrate on our analysis of slower secondary process (β′) and its interpretation. In the relaxation map, we detect the tendency of β′-relaxation to merge with the σ-process and existence of a merging temperature $T_{\beta'}$. However, this feature cannot be considered as the intrinsic evaluation of JG relaxation. In the case of a rigid glass former, the absence of intramolecular degrees of freedom guarantees that slower secondary relaxation is a JG process, by its definition of involving the motion of entire molecule.[10] Here, the slower β′-relaxation for both DES-Li and DES-Na exhibits similar magnitude of activation energies. Moreover, this β′-relaxation displays a stronger temperature dependence on dielectric permittivity. Rivera and Rössler[11] have provided the evidence of secondary relaxations in a series of RTIL based on the same cation: 1-butyal-3-methyl imidazolum (BMIM) with different anions: chloride (Cl), hexafluorophosphate (PF_6), trifluoromethane sulfonateimide (MSF), and bis(trifluoromethane sulphonate)imide (BMSF).[11] It was found that samples with symmetric anions (i.e., Cl, and PF_6) do not display the JG relaxation whereas non-centrosymmetric BMSF show slower secondary relaxation. They proposed that the appearance of this slower JG relaxation is related to the dipole moment of the system. In the present study, both the examined materials are dipolar active which indicate the dipolar nature of JG β′-relaxation.

A remarkable empirical relation of the JG β-relaxation to the glass transition temperature T_g of glass-formers given by $E_\beta \approx 24\ RT_g$ was found by Kudlik *et al.*[35] and valid for many glass formers. This relation is only approximate, nevertheless, there are deviations.[33] The relation between the activation energy of the JG relaxation and T_g of glass formers was derived using coupling model by Ngai,[33]

$$\frac{E_\beta}{RT_g} = 2.303\left(2 - 13.7n - \log_{10}\tau_\infty\right). \quad (12)$$

A series of calculations were performed on a large number of glass formers using Eq. (12) and found large deviation from the empirical relation $E_\beta \approx 24\ RT_g$. For example, calculations

performed on liquid benzoin isobutylether[33] involving JG process show that $\left(\frac{E_\beta}{RT_g}\right)_{expt} = 30.1$ and $\left(\frac{E_\beta}{RT_g}\right)_{theory} = 31.1$. It is worth noting that the present glass formers exhibit thermal behavior of β′-secondary relaxation times with activation energy, DES-Li; $E_{\beta'} = 33.74RT_g$ and DES-Na; $E_{\beta'} = 31.94RT_g$. These experimental observations support the evidence of the JG nature of β′ relaxation.

C. Ac conductivity scaling and time-temperature superposition

In ion-conducting glasses, ion transport originates from thermally activated hopping movements of the mobile ions in the disordered potential landscape.[6] Measurements of electrical conductivity spectra provide the direct information on the hopping dynamics of ions. The scaling property and universality of ac conductivity comes into picture due to the existence of a *characteristic frequency* which systematically depends on temperature. This frequency marks the crossover from long range dc (frequency independent) to ac (frequency dependent) conduction. Subsequently, conductivity scaling allows multiple data sets to collapse on a single locus, suggesting a common physical conduction mechanism irrespective of intensive parameter (i.e., temperature). Moreover, the scaling acts as an important feature in data evaluation and reduces the conduction process into simpler parts for deeper understanding. Frequency-dependent conductivities of disordered ionic materials are best understood with the help of linear response theory.[6] This states that the frequency-dependent electrical conductivity can be directly related to the time-dependent displacements $\langle r^2(t)\rangle$ of the mobile ions in thermal equilibrium and this is translated to scaling behavior of mean square displacement of charge carriers.[63,64] In Figs. 4(a) and 4(b) we present the frequency dependent real part of complex conductivity, σ′(υ) at several temperatures for DES-Li and DES-Na in Log-Log plot. To analyze the conductivity data, we have used the power law model proposed by Jonscher, where the real part of the conductivity can be related to the frequency by $\sigma'(\nu) \propto \nu^n$.[50] Using Almond-West formalism, the real part of the conductivity can be expressed as[50]

$$\sigma(\nu) = \sigma_{dc}\left[1 + \left(\frac{\upsilon}{\upsilon^*}\right)^n\right], \tag{13}$$

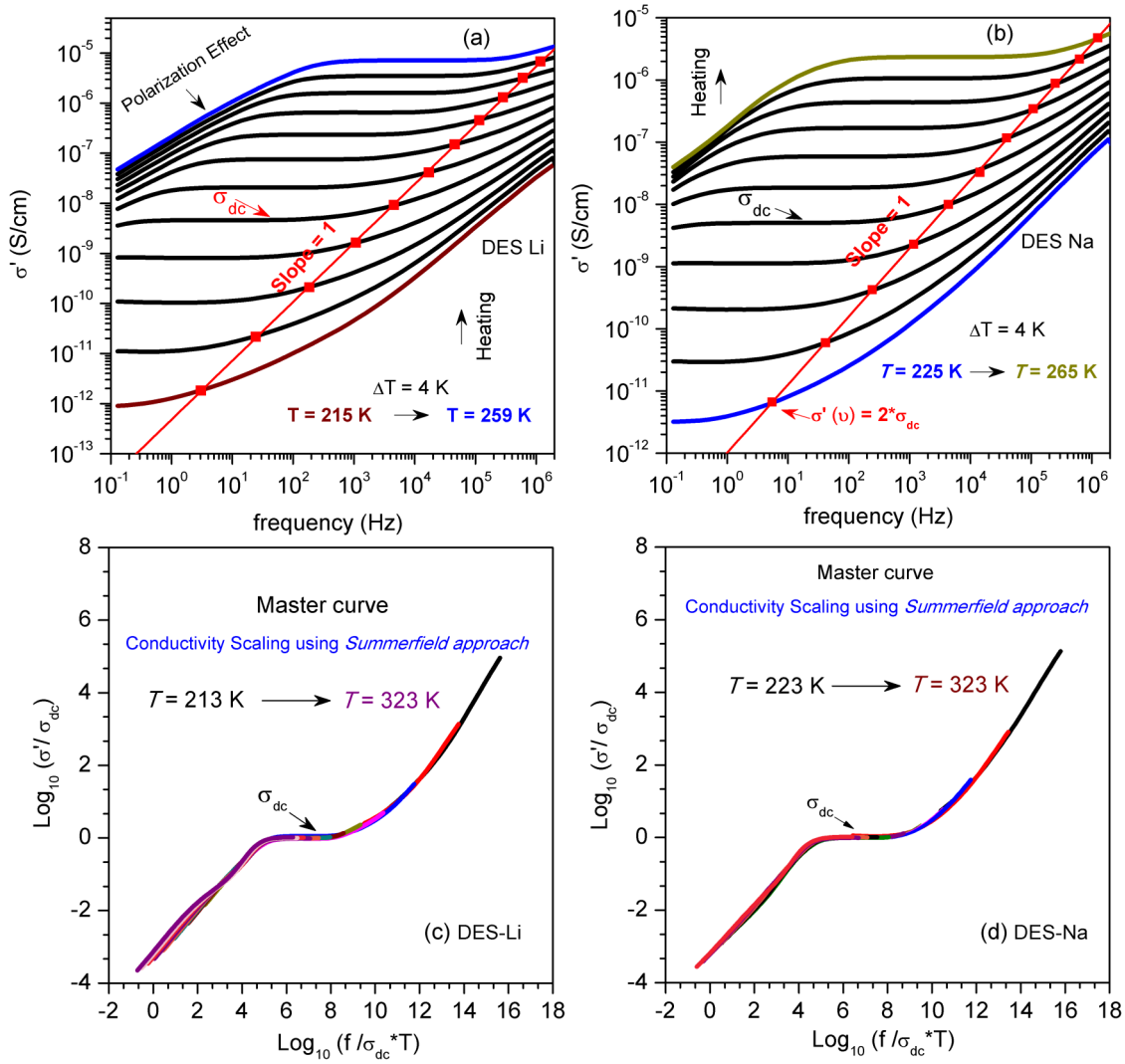

FIG. 4. Frequency dependent conductivity of (a) DES-Li and (b) DES-Na at different temperatures. The red square symbols construct a reference line with slope one, defined by the characteristic frequency, $(\upsilon^*) = 2\sigma_{dc}$. (c) and (d) conductivity master curves using Summerfield scaling approach.

where σ_{dc} corresponds to the dc conductivity, υ^* is the crossover frequency from the dc to the dispersive conductivity, and n is a power law exponent having value less than unity.

The constant part of the conductivity spectra at low frequencies gives the dc conductivity, $\sigma'(\nu) = \sigma_{dc}$ which strongly depends on temperature. This implies that in the long time limit (at low frequencies), the mean square displacement of charge carriers linearly depends on time and the ionic movement is due to random hopping. In the ac regime where conductivity increases with a frequency, mean square displacement becomes nonlinear in time. The onset of conductivity dispersion starts at the characteristic frequency ($\upsilon^* = 2\sigma_{dc}$) and shifts to higher frequency with increasing temperature.[63–65] This characteristic frequency is thermally activated with the same energy as $\sigma_{dc}T$. In a log-log plot, the ac conductivity is much less temperature dependent than the dc conductivity. The ac conductivity spectra at different temperatures can be superimposed into a single master curve by choosing a suitable scaling parameter υ^*. Summerfield proposed a scaling law for the ac conductivity spectra and is represented by[63–65]

$$\frac{\sigma(\upsilon)}{\sigma_{dc}} = F\left(\frac{\upsilon}{\upsilon^*}\right). \tag{14}$$

Here, F is the scaling function that is independent of temperature and υ^* is an individual scaling parameter for each conductivity isotherm. By connecting the crossover frequencies, we obtain a straight line with a slope of one as shown in Figs. 4(a) and 4(b). Here, the conductivity spectra are shifted on both the conductivity and frequency axis to superimpose all $\sigma'(\nu)$ at different temperature spectra to a single curve, the so-called "master curve" as shown in Figs. 4(c) and 4(d). This is usually referred to as the time-temperature superposition principle (abbreviated as TTSP). The master curve indicates the independence of the curve shape on varying temperatures. Several studies have reported the application of this "Summerfield scaling" procedure to the conductivity spectra of ion-conducting glasses.[63–65] The Summerfield scaling method has also an advantage since it uses the directly accessible quantities such as dc conductivity and temperature.

Besides Summerfield approach, a random free energy barrier model (RFEBM) has also been developed by Dyre[66] through hopping conductivity mechanism. According to this model, conduction takes place by hopping of charge carriers in a spatially randomly varying potential landscape. The ac

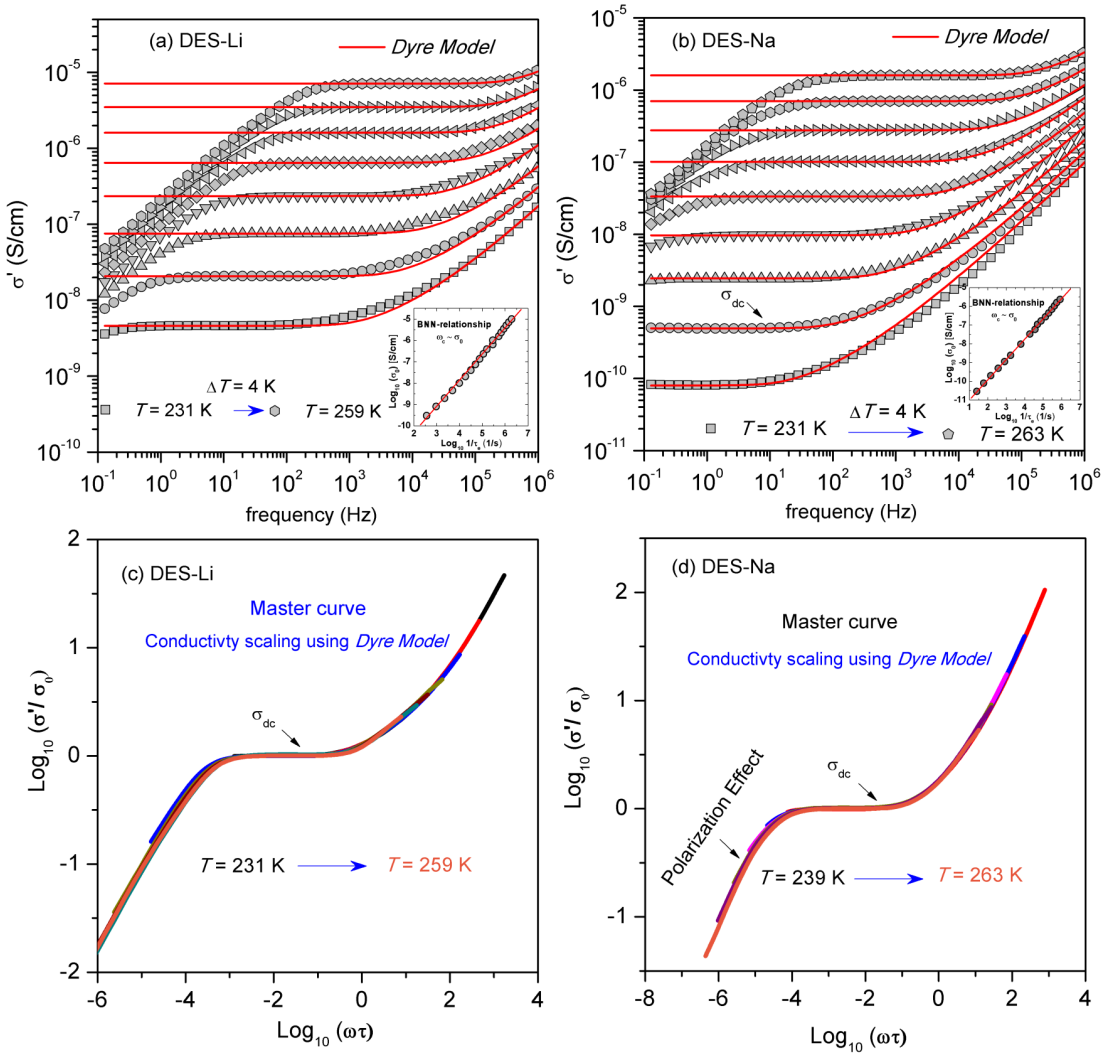

FIG. 5. Frequency dependent conductivity of (a) DES-Li and (b) DES-Na at different temperatures modeled by FERBM. The red lines represent the simulated curve through the experimental data. (Inset—proof of BNN relationship). (c) and (d) Conductivity master curves using Dyre scaling approach.

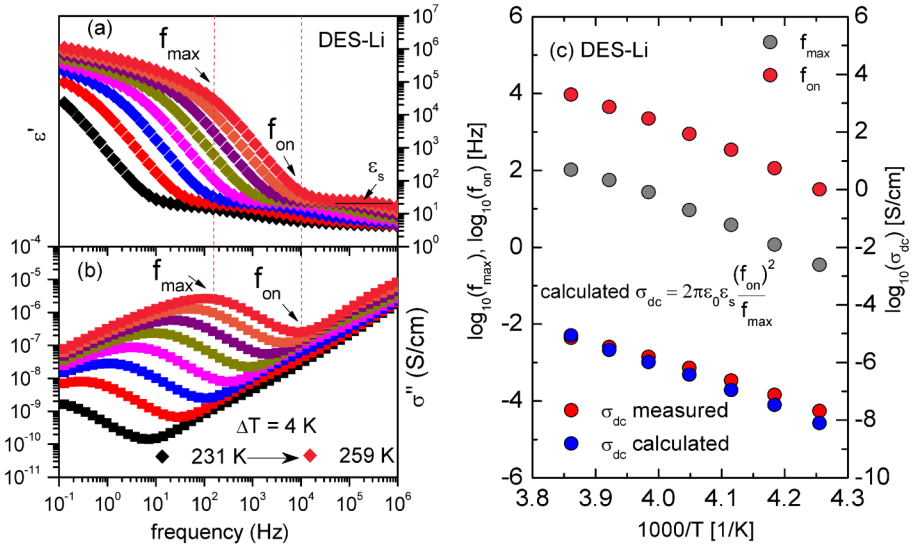

FIG. 6. (a) Real part of permittivity (ε′) and (b) imaginary part of conductivity (σ″) as a function of frequency at several temperatures for DES-Li. The arrows marks, for a particular temperature of 259 K, the frequencies f_{on} (onset of electrode polarization) and f_{max} (maximum development of electrode polarization). (c) f_{on}, f_{max}, calculated σ_{dc}, and measured σ_{dc} as function of 1000/T.

conductivity $\sigma^*(\omega)$ derived under RFEBM[6,50,66] is given by

$$\sigma'(\omega) = \frac{\sigma_0 \omega\tau_e \arctan(\omega\tau_e)}{\frac{1}{4}\ln^2(1+\omega^2\tau_e^2) + (\arctan\omega\tau_e)^2};$$
$$\sigma''(\omega) = \frac{\sigma_0 \omega\tau_e \ln(1+\omega^2\tau_e^2)}{\frac{1}{2}\ln^2(1+\omega^2\tau_e^2) + 2(\arctan\omega\tau_e)^2}, \quad (15)$$

where τ_e is the attempt to frequency to overcome the largest barrier determining the dc conductivity.

Fittings were carried using Eq. (15) which describes frequency and temperature dependence with only two adjustable parameters, i.e., σ_0 and τ_e. Figs. 5(a) and 5(b) represent the conductivity spectra modeled using RFEBM for DES-Li and DES-Na, respectively. From the fits, the dc conductivity (σ_0) and relaxation time (τ_e) are obtained. In order to understand the possibility of ac conductivity scaling, we have plotted normalized conductivity $\left(\frac{\sigma'}{\sigma_0}\right)$ with respect to normalized frequency $\left(\frac{\omega}{\omega_e}\right)$. It is observed that all the conductivity spectra within temperature range T = 230 K to T = 265 K fall into a single locus for the examined materials as shown in Figs. 5(c) and 5(d). Therefore, construction of master curve is possible using Dyre model. The frequency ω_e also satisfies Barton-Nakajima-Namikawa (BNN)[6,50] relation which suggests that $\sigma'(\omega \to 0) \sim \omega_e$. As shown in Figs. 5(a) and 5(b) [inset], the BBN relation is well fulfilled. It indicates that dc and ac conduction mechanism is based on the same mechanism of transport.

For higher temperature and at low frequencies, we observed polarization effect typically observed in ion-conducting materials. The most prominent features of electrode polarization are noticed in real part of permittivity (ε′) and imaginary part of conductivity (σ″(ν))[67] representations as shown in Fig. 6. The onset of space charge effect starts at a certain frequency f_{on} which is witnessed by a sharp increase in ε′ and a minima in σ″(ν) (for a certain temperature at 259 K of DES-Li). At a particular frequency f_{max}, full development of the electrode polarization takes place with a maximum in σ″(ν) and a plateau in ε′. In order to understand the effect of space charge polarization on conductivity scaling, we have plotted the f_{max}, f_{on}, and the dc-conductivity as a function of 10^3/T. We found that the characteristic frequencies (f_{max} and f_{on}) related to space charge effect, measured σ_{dc}, and calculated $\sigma_{dc} = 2\pi\varepsilon_0\varepsilon_s\varepsilon_0\frac{(f_{on})^2}{f_{max}}$[67] scale similarly with temperature. Similar types of observations are also witnessed for DES-Na.

IV. SUMMARY AND CONCLUSIONS

On the basis of dielectric data which provide the direct access to the molecular dynamic features, collected for the present deep eutectic solvents, we have drawn the following conclusions.

(a) Complex modulus spectroscopy is an appropriate representation of dielectric data to understand the key features of conductivity relaxation in the ionic melts and its role on physical explanation for the origin of secondary relaxation process. Comparative analyses involving ionic mobility contribution to conductivity relaxation and glass transition have also been discussed.

(b) Using Ngai's coupling model, we have successfully established the basis of secondary relaxation process. The existence of the intrinsic JG relaxation phenomenon involving long range Coulomb interactions and re-orientation of dipoles has been taken into account to elucidate the nature of the localized processes in the present molten ionic systems. In case of rigid glass former, it has been well established that the slower process one is of JG kind. Since the rigid acetamide unit has no internal degrees of freedom, therefore, its origin does not contribute to the β″-fast relaxation process. The character of high frequency beta process mirrors the primitive conductivity relaxation and carries identical information. Ultimately, the conductive nature of the fast secondary process suggests the JG involvement due to the definition of ion-transport at thermal equilibrium which always entails intermolecular feature. So the present glass former is a special case where we observe primary conductivity, slower dipolar β′-JG, and faster conductivity β″-JG relaxation.

(c) Again in conductivity representation, we do not observe JG-conductivity feature due to the substantial dominance

of NCL component over this process at low temperature. The NCL behavior, appearing at high frequencies/short times when molecules are caged, is terminated by the onset of the JG β-conductivity relaxation. On the contrary, modulus representation describes the relaxation in reciprocal space which amplifies localized process.

(d) The Summerfield approach and free energy random barrier model allow us to construct the master curves in conductivity representation and support TTSP principle. This implies that conduction mechanism is independent of temperature.

Therefore, the present study of conductivity relaxation of the ionic melt and its implications on theoretical interpretation have fundamental importance on the study of the glass transition dynamics of ionic melts. This type of interesting observation on secondary relaxation process and scaling is rather intriguing and needs to be addressed by further experimental investigation.

ACKNOWLEDGMENTS

Authors would like to acknowledge Professor K. L. Ngai and Dr. S. Hensel-Bielowka for fruitful suggestion to the manuscript. Authors are deeply grateful for the financial support by the National Science Centre within the framework of the Maestro2 project (Grant No. DEC-2012/04/A/ST3/00337). H.S. is grateful to the Tokyo Ohka Foundation for the Promotion of Science and Technology for the financial support.

[1]C. A. Angell, K. L. Ngai, G. B. McKenna, P. F. McMillan, and S. W. Martin, J. Appl. Phys. **88**, 3113 (2000).
[2]M. D. Ediger, C. A. Angell, and S. R. Nagel, J. Phys. Chem. **100**, 13200 (1996).
[3]K. L. Ngai and C. Leon, Phys. Rev. B **60**, 9396 (1999).
[4]C. M. Roland, S. H. Bielowka, M. Paluch, and R. Casalini, Rep. Prog. Phys. **68**, 1405 (2005).
[5]M. D. Ediger and P. Harrowell, J. Chem. Phys. **137**, 080901 (2012).
[6]F. Kremer and A. Schoenhals, *Broadband Dielectric Spectroscopy* (Springer, Berlin, 2003).
[7]G. Floudas, M. Paluch, A. Grzybowski, and K. L. Ngai, *Molecular Dynamics of Glass Forming Systems, Effect of Pressure* (Springer, New York, 2011), Chap. 6.
[8]C. A. Angell, Y. Ansari, and Z. Zhao, Faraday Discuss. **154**, 9 (2012).
[9]K. L. Ngai, J. Phys.: Condens. Matter **15**, S1107 (2003).
[10]K. L. Ngai and M. Paluch, J. Chem. Phys. **120**, 857 (2004).
[11]A. Rivera and E. A. Rössler, Phys. Rev. B **73**, 212201 (2006).
[12]Z. Wojnarowska, Y. Wang, J. Pionteck, K. Grzybowska, A. P. Sokolov, and M. Paluch, Phys. Rev. Lett. **111**, 225703 (2013).
[13]Z. Wojnarowska, J. Knapik, M. Díaz, A. Ortiz, I. Ortiz, and M. Paluch, Macromolecules **47**, 4056 (2014).
[14]Z. Wojnarowska, C. M. Roland, K. Kolodziejczyk, A. Swiety-Pospiech, K. Grzybowska, and M. Paluch, J. Phys. Chem. Lett. **3**, 1238 (2012).
[15]Q. Zhang, K. O. Vigier, S. Royer, and F. Jerome, Chem. Soc. Rev. **41**, 7108 (2012).
[16]A. Boisset, S. Menne, J. Jacquemin, A. Balducci, and M. Anouti, Phys. Chem. Chem. Phys. **15**, 20054 (2013).
[17]E. L. Smith, A. P. Abbott, and K. S. Ryder, Chem. Rev. **114**, 11060 (2014).
[18]S. Keskin, D. Talay, U. Akman, and O. Hortacsu, J. Supercrit. Fluids **43**, 150 (2007).
[19]H. Zhaoa and G. A. Baker, J. Chem. Technol. Biotechnol. **88**, 3 (2013).
[20]D. R. MacFarlane *et al.*, Energy Environ. Sci. **7**, 232 (2014).
[21]A. P. Abbott, G. Capper, D. L. Davies, and R. K. Rasheed, Chem. - Eur. J. **10**, 3769 (2004).
[22]A. P. Abbott, K. E. Ttaib, G. Frisch, K. J. McKenzie, and K. S. Ryder, Phys. Chem. Chem. Phys. **11**, 4269 (2009).
[23]G. Berchiesi, M. D. Angelis, G. Rafaiani, and G. Vitali, J. Mol. Liq. **51**, 11 (1992).
[24]G. Berchiesi, G. Rafaiani, G. Vitali, and F. Farhat, J. Therm. Anal. **44**, 1313 (1995).
[25]G. G. Lobbia and G. Berchiesi, Thermochim. Acta **74**, 251 (1984).
[26]G. Kalita, K. G. Sarma, and S. Mahiuddin, J. Chem. Eng. Data **44**, 222 (1999).
[27]R. A. Wallace, Inorg. Chem. **11**, 414 (1972).
[28]S. Capaccioli, K. Kessairi, M. Shahin Thayyil, D. Prevosto, and M. Lucchesi, J. Non-Cryst. Solids **357**, 251 (2011).
[29]U. Schneider, R. Brand, P. Lunkenheimer, and A. Loidl, Phys. Rev. Lett. **84**, 5560 (2000).
[30]M. Paluch, C. M. Roland, S. Pawlus, J. Zioło, and K. L. Ngai, Phys. Rev. Lett. **91**, 115701 (2003).
[31]G. P. Johari and M. Goldstein, J. Chem. Phys. **53**, 2372 (1970).
[32]G. P. Johari and M. Goldstein, J. Chem. Phys. **55**, 4245 (1971).
[33]K. L. Ngai and S. Capaccioli, Phys. Rev. E **69**, 031501 (2004).
[34]K. Kaminski, E. Kaminska, M. Paluch, J. Ziolo, and K. L. Ngai, J. Phys. Chem. B **110**, 25045 (2006).
[35]A. Kudlik, S. Benkhof, T. Blochowicz, C. Tschirwitz, and E. Rossler, J. Mol. Struct. **479**, 201 (1999).
[36]K. L. Ngai, J. Non-Cryst. Solids **353**, 4237 (2007).
[37]K. L. Ngai, J. Non-Cryst. Solids **353**, 709 (2007).
[38]G. Jarosz, M. Mierzwa, J. Ziozo, M. Paluch, H. Shirota, and K. L. Ngai, J. Phys. Chem. B **115**, 12709 (2011).
[39]H. K. Kashyap and R. Biswas, J. Phys. Chem. B **114**, 254 (2010).
[40]A. Das, S. Das, and R. Biswas, Chem. Phys. Lett. **581**, 47 (2013).
[41]B. Guchhait *et al.*, J. Chem. Phys. **140**, 104514 (2014); **136**, 174503 (2012).
[42]R. Biswas, A. Das, and H. Shirota, J. Chem. Phys. **141**, 134506 (2014).
[43]A. Amico, G. Berchiesi, C. Cametti, and A. D. Biasio, J. Chem. Soc., Faraday Trans. 2 **83**, 619 (1987).
[44]G. Berchiesi *et al.*, J. Mol. Liq. **83**, 271 (1999); **54**, 103 (1992).
[45]I. M. Hodge, K. L. Ngai, and C. T. Moynihan, J. Non-Cryst. Solids **351**, 104 (2005).
[46]C. T. Moynihan, Solid State Ionics **105**, 175 (1998).
[47]R. Kohlrausch, Ann. Phys. (Leipzig) **72**, 393 (1847).
[48]G. Williams and D. C. Watts, Trans. Faraday Soc. **66**, 80 (1970).
[49]N. G. McCrum, B. E. Read, and G. Williams, *Anelastic and Dielectric Effects in Polymeric Solids* (Dover, New York, 1991).
[50]J. C. Dyre, P. Maass, B. Roling, and D. Sidebottom, Rep. Prog. Phys. **72**, 046501 (2009).
[51]S. Havriliak and S. Negami, Polymer **8**, 161 (1967).
[52]H. Vogel, Phys. Z. **22**, 645 (1921).
[53]G. S. Fulcher, J. Am. Ceram. Soc. **8**, 339 (1925).
[54]G. Tammann and W. Hesse, Z. Anorg. Allg. Chem. **156**, 245 (1926).
[55]M. Paluch, Z. Wojnarowska, and S. Hensel-Bielowka, Phys. Rev. Lett. **110**, 015702 (2013).
[56]F. Mizuno, J. Belieres, N. Kuwata, A. Pradel, M. Ribes, and C. A. Angell, J. Non-Cryst. Solids **352**, 5147 (2006).
[57]F. Senti and D. Harker, J. Am. Chem. Soc. **62**, 2008 (1940).
[58]R. D. Shannon and C. T. Prewitt, Acta Crystallogr., Sect. B: Struct. Crystallogr. Cryst. Chem. **25**, 925 (1969).
[59]R. J. Klein, S. Zhang, S. Dou, B. H. Jones, R. H. Colby, and J. Runt, J. Chem. Phys. **124**, 144903 (2006).
[60]D. M. Laughman, R. D. Banhatti, and K. Funke, Phys. Chem. Chem. Phys. **12**, 14102 (2010).
[61]C. León, A. Rivera, A. Várez, J. Sanz, and J. Santamaria, Phys. Rev. Lett. **86**, 1279 (2001).
[62]K. L. Ngai, R. W. Rendell, and C. Leon, J. Non-Cryst. Solids **307**, 1039 (2002).
[63]B. Roling, A. Happe, K. Funke, and M. D. Ingram, Phys. Rev. Lett. **78**, 2160 (1997).
[64]D. L. Sidebottom, Phys. Rev. Lett. **82**, 3653 (1999).
[65]S. Das and A. J. Bhattacharyya, J. Phys. Chem. Lett. **3**, 3550 (2012).
[66]J. C. Dyre, J. Appl. Phys. **64**, 2456 (1988).
[67]A. Serghei, M. Tress, J. R. Sangoro, and F. Kremer, Phys. Rev. B **80**, 184301 (2009).